A Facile Direct Spray-coating of Pebax® 1657: Towards Large-scale Thin-film Composite Membranes for Efficient CO_2/N_2 separation

Xu Jiang[a], Chong Yang Chuah[a], Kunli Goh[a], Rong Wang[ab]*

[a] Singapore Membrane Technology Centre, Nanyang Environment and Water Research Institute, Nanyang Technological University, 1 Cleantech Loop, 637141, Singapore

[b] Singapore of Civil and Environmental Engineering, Nanyang Technological University, 50 Nanyang Avenue, 639798, Singapore

* Corresponding author at: Singapore Membrane Technology Centre, Nanyang Environment and Water Research Institute, Nanyang Technological University, 1Cleantech Loop, 637141, Singapore.

E-mail address: rwang@ntu.edu.sg (R. Wang).

Abstract

High-efficient CO_2 capture using membrane separation technology is a promising approach towards environmental redemption in recent years. Thin-film composite (TFC) membrane with selective layer made of CO_2-philic materials is the preferred membrane type for industrial-scale application, owing to its high permselectivity and good processability. Herein, we propose a facile direct spray-coating method to fabricate Pebax® 1657 thin-film on a porous polysulfone (PSF) substrate. Unlike most conventional multilayer TFC membranes, the unnecessary need for gutter layer in this work greatly simplifies the membrane fabrication process. Pebax® 1657 thin films were deposited through direct spraying of the polymer solution containing Pebax® 1657 on PSF substrate under ambient temperature. The as-prepared Pebax®1657 TFC membranes showed decent separation performances with CO_2 permeance of >200 GPU and CO_2/N_2 selectivity of >50 for mixed gas (vol. (CO_2)/vol. (N_2) =20/80) tests. The facile TFC membrane fabrication and good CO_2 separation performances make the direct spray coated Pebax®1657 membranes a promising strategy for large-scale CO_2 capture applications.

Key words: Membrane separation**,** CO_2 capture, thin-film composite, Pebax® 1657, spray-coating

1. Introduction

The ever-increasing CO_2 level in the atmosphere has brought unprecedented impacts and challenges to global environment protection and sustainability in recent decades [1, 2]. There is now a great demand for clean energy and environmental redemption technology given that fossil fuel is still expected to last over 20 years as main energy resource. Developing high-efficient carbon capture and storage (CCS) technologies is a consensual solution to reduce CO_2 emissions and mitigate the negative effects causing climate change [3, 4].

As a clean and low carbon footprint technology, membrane-based CO_2 separation has attracted a lot of attention and showed great potential for large-scale CO_2 capture [5-7]. The development of high-performance CO_2 separation membranes can be divided into two parts: seeking suitable membrane materials and developing membrane fabrication process that is facile for scaling-up. According to the solution-diffusion theory, the CO_2 transport efficiency can be increased by leveraging the high CO_2 solubility of rubbery polymers [8]. On this note, ideal materials for CO_2 separation membranes should be CO_2-philic, which include Poly (ethylene oxide) (PEO)-containing materials, reactive carriers in facilitated transport membranes (FTMs) [9, 10], and functional porous materials with molecular sieve capacity (e.g., metal-organic frameworks, covalent-organic frameworks, and graphene oxides, etc.) [11-15] Although the performance upper limit of FTMs is higher, there are multiple drawbacks associated with FTMs, including carrier leakages [10], carrier oxidation [16], humidity-dependence performances [17], and membrane stability that remains to date controversial. Similarly, molecular sieve membranes show high-efficient gas transport due to the fast pressure-driven gas diffusion in narrow channels, but they are still challenged by several key issues regarding large-scale fabrication, technical viability as well as high cost of production at the current stage [18-20]. On the other hand, PEO-based membranes are attractive, owing to the very high CO_2 solubility and theoretical CO_2/gas selectivity as a result of "dipole-quadrupole" interactions between ethylene oxide (EO) units and CO_2 molecules [21]. However, pure PEO-containing materials are unfavorable due to their semi-crystalline nature and poor

mechanical properties [22]. Crosslinking [21], blending [23], grafting [24], and compositing [25] are frequently-used strategies to synthesize highly-permeable amorphous PEO-based membranes [26]. In recent decades, PEO-containing block copolymers are preferred, owing to their excellent mechanical stability and processability. Several commercial PEO-containing copolymers include Pebax® [27, 28], Polaris™ [29, 30], and PolyActive™ [31] have been developed and showed high capacity for CO_2 separation membrane fabrication both in lab-scale and industrial-scale.

Apart from selecting the right materials, engineering the thickness of the membrane is also essential [32]. The membrane must be sufficiently thin to reduce mass transfer resistance so as to increase the CO_2 permeance [33, 34]. Currently, a multilayer thin-film composite (TFC) membrane, comprising a porous substrate layer, a dense and highly permeable gutter layer, and an ultrathin selective layer ($\leq$1 μm), is the most compelling design for high-performance gas separation membranes [35-37]. Most TFC membranes are fabricated using top-down approaches, including dip coating, spin coating, and doctor-blade casting, through which the polymer cast solution is uniformly coated on the substrate to form an ultrathin top layer [38]. Particularly, dip coating is the most favorable method for industrial-scale TFC membranes manufactured at the current stage, which have realized the roll-to-roll fabrication of flat sheet membranes and small-scale production of hollow fiber modules [39-42]. To use these approaches, a gutter layer is almost always required to prevent polymer intrusion into the pores of the substrate [43, 44]. Polymeric TFC membranes fabricated without gutter layers usually show very low gas permeance of several or dozens of GPU due to the serious polymer intrusion [45-48]. This gutter layer is made of highly permeable but less selective materials. For example, polydimethylsiloxane (PDMS) is a frequently used material for the gutter layer due to its high intrinsic permeability. However, the inert and low surface energy of PDMS can reduce adhesion strength with the top selective layer, rendering defect-free selective layer formation a challenge and scaling-up TFC membranes become difficult[34].

Apart from the above-mentioned methods, spray coating is an alternative and attractive

technique for thin film deposition, which has been adopted to fabricate polymer selective layers [49-51], assembled multilayer polyelectrolyte membranes [52-54], and deposited thin layer of nanomaterials on membrane substrates for liquid filtration and gas separation [55-58]. Compared to dip coating or blade casting, the atomized solvent of the sprayed liquid evaporates more quickly, which allows a fast curing of the coating layer, and thus a reduction in the intrusion of sprayed liquid into the substrate when directly sprayed on a porous substrate. This makes gutter-free fabrication of high permeable TFC membrane possible. Moreover, spray coating has the same advantage of depositing thin film on a large area as dip coating due to its simple operation. Therefore, to enhance TFC membrane scalability, in current work, we developed a straightforward strategy to fabricate Pebax® thin-film on a porous substrate via a direct spray-coating method. Diluted Pebax® solution was directly sprayed on the surface of a bare polysulfone (PSF) ultrafiltration membrane using an air brush. As compared to conventional methods, this direct spray strategy is much more facile as it eliminates the need for a gutter layer, which greatly simplifies the entire TFC membrane formation process. The CO_2 permeance and CO_2/N_2 selectivity of the as-prepared Pebax® TFC membranes can reach over 200 GPU and 50 with good long-term stability for mixed gas tests, respectively. The CO_2 permeance of our directly sprayed TFC membrane is significantly higher than other gutter-free Pebax® TFC membranes due to less polymer intrusion as a result of the quick vaporization of the highly atomized solvent during the spraying process. Furthermore, the sprayed Pebax® TFC membrane can be easily scaled-up to A4-size in laboratory conditions, demonstrating the great potential of our direct spray-coating method for manufacturing of industrial-scale CO_2 separation membranes.

2. Experimental

2.1 Materials

Pebax®1657 in pellet form was purchased from Arkema Pte. Ltd. Polysulfone (PSF, Solvay P-3500) was obtained from Solvay. PET nonwoven fabrics (E055094-74) was provided by

MIKI & CO., Ltd, Japan. Ethanol (EtOH, 97%), methanol (99%), n-hexane (99%), and dimethyl formamide (DMF, EMSURE®) were supplied by Sigma-Aldrich and used as-received. Sylgard®-184 (elastomeric polydimethylsiloxane (PDMS) kit) consisting of a silicone elastomer (part A) and a cure agent (part B) was purchased form Dow Corning Pte. Ltd. High purity (99.999%) helium and mixed gas CO_2/N_2 (v/v=20/80) was obtained from Air Liquide Pte. Ltd.

2.2 Preparation of porous PSF substrate

Flat sheet PSF ultrafiltration substrate was fabricated using a classic nonsolvent-induced phase inversion method. The details can be found elsewhere[59]. Typically, PSF pellets were dried in vacuum over night at 80 ℃ before use. Then a 17 wt.% PSF casting solution were prepared by dissolving a certain amount of PSF in DMF at 70 ℃ under vigorous stirring for 24 hours. The obtained homogeneous casting solution was cooled to room temperature and degassed by vacuum pump for 24 hours to eliminate air bubbles.

The membrane formation was performed on an automatic casting machine at a casting speed of 4 m/min. During the casting, the polymer solution was continuously poured into the gap (200 μm) between the settled casting knife and nonwoven fabric. The casted membrane was transferred into a water coagulating bath (25 ℃) to induce the phase inversion. The as-prepared PSF substrate was then cut into A4 size and soaked in fresh deionized (DI) water (refreshed every 12 hours) for 48 hours to ensure complete removal of the residual DMF.

Before drying, a solvent exchange process was carried out to prevent collapse of the porous structure of PSF membranes. The PSF substrates were taken out from DI water and immediately immersed in fresh methanol for 30 min, and then transferred to fresh n-hexane for another 30 min. After solvent-exchange, PSF substrates were dried in air overnight, followed by vacuum drying at 60 ℃ for 24 hours.

2.3. Preparation of Pebax® 1657 dense membrane

Dense Pebax® membrane was prepared by solvent evaporation method. Typically, 0.5 g Pebax®1657 was dissolved in 100 mL EtOH/Water (v/v=7/3) mixed solvent at 70 ℃ for 6 hours to obtain a homogeneous polymer casting solution. After filtering by a stainless-steel mesh (7 μm) and degassed by ultrasonication for 10 min, the casting solution was carefully poured into a glass petri dish. The petri dish was covered by an aluminum foil with reserved pinholes to allow slow evaporation of the solvent at ambient temperature for 24 hours. Thereafter, the solidified Pebax® dense membrane was carefully peeled off, followed by vacuum drying at 80 ℃ for 24 hours.

2.4 Spray coating of thin-film composite membranes

Pebax®1657 pellets were firstly dissolved in EtOH/Water (v/v=7/3) mixed solvent at 70 ℃ under stirring to prepare a polymer solution at a concentration of 5 mg/mL. Before spraying, the polymer solution was diluted to a certain concentration as needed, followed by ultrasonication for 10 minutes to remove air bubbles. The spray coating was carried out by a handheld air brush (Holder HD-130) with a 0.2 mm spray nozzle. The compressed air is supplied by a mini air compressor (HS-AS08S) with an air flow of 10.5 L/min and a operation presssure range of 2-14.7 psi . As shown in **Scheme 1**, the PSF substrate was cut into a 4×4 cm piece and fixed onto a tilted (45°) Teflon plate with masking tapes. The distance between spray nozzle and PSF substrate was kept at 10 cm. The spray was manually performed at a pressure of 14.7 psi and a liquid flux of 0.25 mL/min. To ensure a uniform coating, the spray was carried out in a continuous left-to-right-to-left motion, inching slowly across the entire length of the substrate. Meanwhile, the tilted substrate was clockwise roated 90 ° along the x-y plane at intervals to ensure the spray uniformity in every direction of the substrate. After spraying, the membrane was dried in air for 12 hours and then dried in vacuum oven for another 24 hours at 80 ℃ before tests. The as-prepared membranes were denoted as **SC-PEBA*a*$_{b}$**, where the numeric *a* represents the concentration of Pebax® solution, *b* represents the spray volume. For example, SC-PEBA1$_{0.5}$ means that the membrane was fabricated by spraying 0.5 mL of 1mg/mL Pebax® solution on a 16 cm^2 PSF substrate.

For some Pebax® TFC membranes, a further PDMS spray coating was carried out after sufficient drying of the Pebax® layer. For this spray, 0.1 wt.% PDMS solution was prepared by dissolving certain amount of Sylgard® 184 part A and part B mixture (10/1 by mass) in *n*-hexane. The prepared PDMS solution was pre-crosslinked at 60 ℃ for 3 hours before spray. The spray process followed the above-mentioned procedure for Pebax® spray-coating. Spray volume was fixed at 1 mL for each membrane. The obtained membranes were denoted as **SC-PEBA*a*$_b$-PDMS**, which were further dried at 60 ℃ for 24 hours to ensure the total crosslinking of the PDMS.

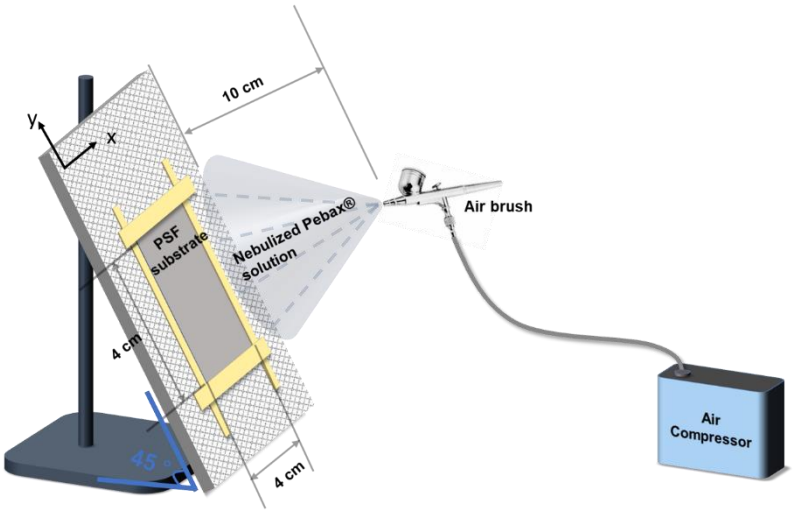

Scheme 1. Schematic of spray coating of Pebax® on PSF substrate via air brush.

2.5 Characterization

The chemical structures of PSF substrate and the as-prepared thin films were characterized by attenuated total reflection infrared (ATR-IR) spectra using a Shimazu IRPrestige-21 spectrometer. Membrane surface and cross-sectional morphologies were observed through a scanning electron microscope (JEOL JSM-7200F). Water contact angle of different surfaces were measure by a goniometer (Dataphysics OCA 15).

2.6 Gas permeation tests

Mixed gas (CO_2/N_2) separation performance tests of the as-prepared membranes were

conducted on a lab-scale Wicke−Kallenbach permeation setup (GTR-11A, Japan) (**Fig. S1**). The effective test area of the permeation cell is 1.766 cm^2. Generally, CO_2/N_2 (20/80) mixed gas was fed to the membrane surface, while pure Helium (He) was used as a sweep gas at the permeate side to carry the permeate gas to a gas chromatography (Shimadzu GC-2014) with thermal conductivity detector (TCD) for composition analysis. The flow rates were set by two mass flow controllers on the feed and permeate sides. The flow rate of feed gas (200 ml/min) was set higher than the permeate/sweep gas (50 mL/min) and the gas permeation rate to prevent back permeation and concentration polarization [60, 61]. The total flux of the permeate gas was measured by a bubble flow meter. All tests were carried at 25 ℃. Feed gas pressure was adjusted from 1–10 bar.

3. Results and Discussion

3.1 Membrane morphology analysis

The surface of PSF UF substrate used in this work is highly porous with uniformly distributed ~20 nm-width pores (**Fig. S2a**). The surface porosity as calculated from the SEM images is ~26.4%. The cross-section reveals a dominant sponge-like structure of the PSF substrate with a thickness of 50 μm (**Fig. S2b**).

The top surface SEM images of Pebax® spray coated TFC membranes are depicted in **Fig. 1**. After Pebax® coating, the surface pores of the PSF substrates are almost blocked. At low spray volume and low Pebax® concentration, the membrane surface may not be sufficiently covered since pinholes and defects remain visible on SC-PEBA$1_{0.25}$ (**Fig. 1a**). Unlike dip coating or doctor-blade casting, spray coating is a more dynamic process, during which fast evaporation of the solvent is occurring while the membrane surface undergoes continuous spraying. This results in rough and undulating surfaces for all sprayed membranes.

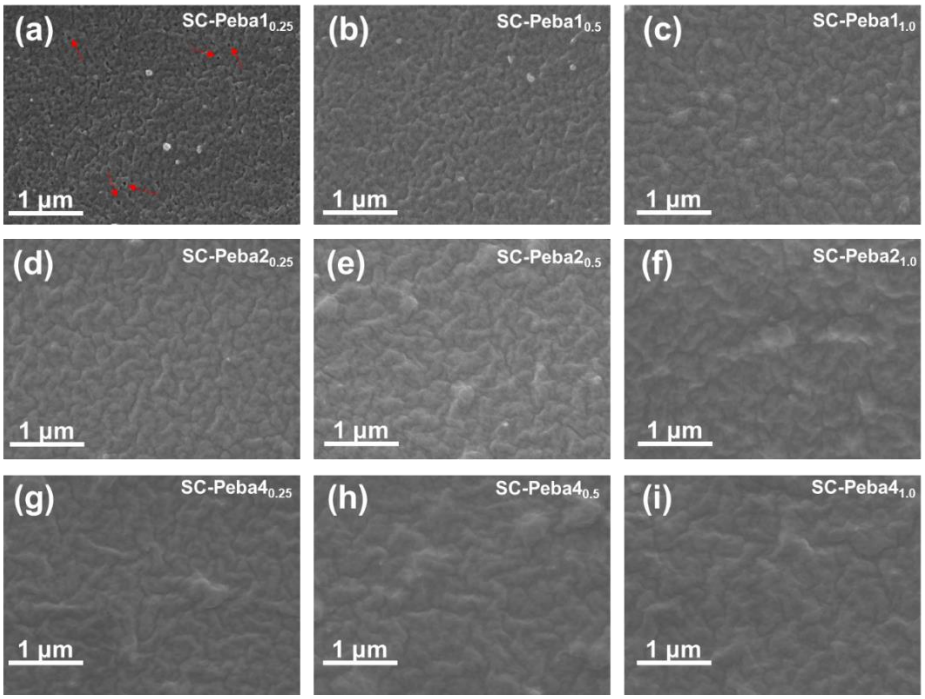

Fig.1. Surface SEM images of sprayed membranes at different spray volumes and Pebax® concentrations. (a) SC-PEBA1$_{0.25}$ (pinholes are highlighted by red arrows), (b) SC-PEBA1$_{0.5}$, (c) SC-PEBA1$_{1.0}$, (d) SC-PEBA2$_{0.25}$, (e) SC-PEBA2$_{0.5}$, (f) SC-PEBA2$_{1.0}$, (g) SC-PEBA4$_{0.25}$, (h) SC-PEBA4$_{0.5}$, (i) SC-PEBA4$_{1.0}$.

Fig. 2 shows the cross-sectional SEM images of the sprayed membranes. Since no gutter layer was used between the sprayed Pebax® layer and PSF substrate in this work, the intrusion of Pebax® solution into the pores of PSF substrate is inevitable. As a result, the top layer cannot be clearly distinguished from the PSF substrate at low Pebax® concentration of 1 mg/mL due to spray solution intrusion. In association with the surface SEM image (Fig. 1a), it indicates that the TFC membrane sprayed with low concentration solution might be defective. At higher Pebax® concentrations of 2 mg/mL and 4 mg/mL, a dense top layer of different thickness can be observed. Meanwhile, comparing the two membranes sprayed by the same net amount of Pebax®, for example SC-PEBA2$_{1.0}$ and SC-PEBA4$_{0.5}$ both containing 2 mg Pebax®, the top layer thickness of SC-PEBA4$_{0.5}$ (418 nm) is significantly higher than that of SC-PEBA2$_{1.0}$ (231 nm), which indicates that higher Pebax® concentration facilitates a reduction in solution intrusion due to the higher viscosity. The apparent top layer thicknesses of TFC membranes

sprayed with 2 mg/mL and 4 mg/mL Pebax® solution, as summarized in Fig. 3, are measured from SEM images for relative comparison. Notably, the apparent thickness is not the actual value because of the uncertainty associated with the intrusion depth of the Pebax® solution. Besides, the manual spraying operation does not guarantee uniformity of the coating layer. Consequently, the apparent top layer thickness of the TFC membrane increases with the concentration and spray volume of the Pebax® solution, albeit the relations are not strictly linear.

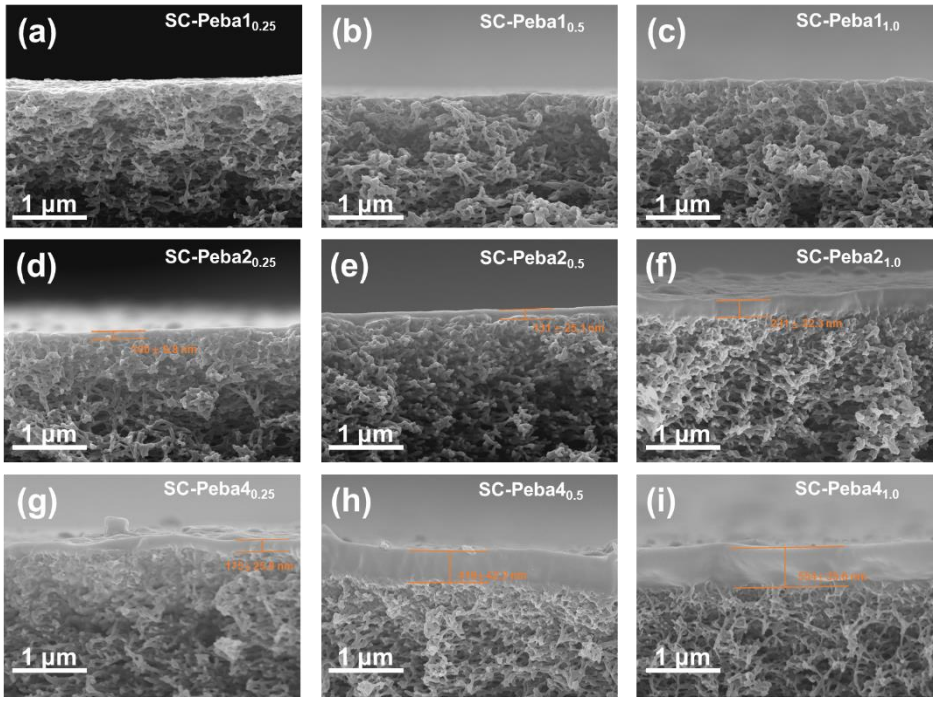

Fig.2. Cross-sectional SEM images of sprayed membranes at different spray volumes and Pebax® concentrations. (a) SC-PEBA1$_{0.25}$, (b) SC-PEBA1$_{0.5}$, (c) SC-PEBA1$_{1.0}$, (d) SC-PEBA2$_{0.25}$, (e) SC-PEBA2$_{0.5}$, (f) SC-PEBA2$_{1.0}$, (g) SC-PEBA4$_{0.25}$, (h) SC-PEBA4$_{0.5}$, (i) SC-PEBA4$_{1.0}$.

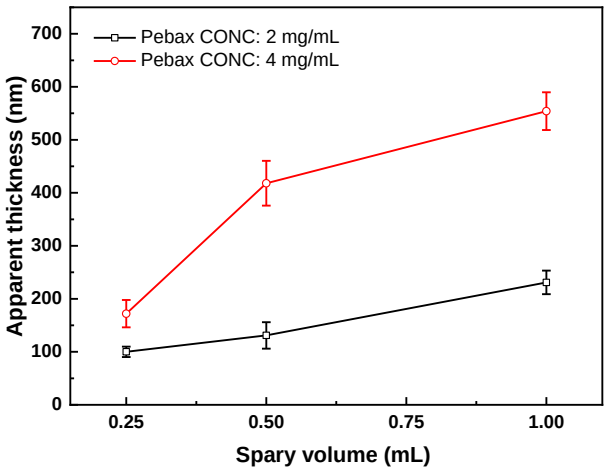

Fig. 3. Apparent thicknesses of sprayed membranes measured from SEM images.

3.2 Configurations of the sprayed TFC membranes.

The chemical composition of the bare PSF substrate and sprayed membranes were investigated by ATR-FTIR (**Fig. 4a**). For the bare PSF substrate, a sharp band at 1241 cm^{-1} is caused by the stretching vibration of Ph-O-Ph, while the bands located at 1485 cm^{-1} and 1578 cm^{-1} are attributed to the stretching vibration of benzene rings [62]. Additionally, the S=O symmetric stretching is observed at 1150 cm^{-1} [63]. The spectra of spray-coated membrane show several differences as compared to the bare PSF. Accordingly, after Pebax® coating, the new characteristic bands at 1102 cm^{-1}, 1635 cm^{-1}, 1730 cm^{-1}, and 3300 cm^{-1} indicate the presence of C-O-C, HN-C=O, O-C=O, and -N-H- functional groups [27, 64], respectively, confirming the successful coating of Pebax®1657. With further PDMS coating, the vibration bands of Si-O-Si (1100-1000 cm^{-1}), Si-CH_3 (1255 cm^{-1}), and -CH_3 (2963 cm^{-1}) are observed correspondingly[65].The successful spray-coating of Pebax® and PDMS were also verified by the changes in water contact angles (**Fig. 4b**). With Pebax® coating, the water contact angle decreased from 92.5±2.4° of bare PSF to 45.0±1.6° due to the intrinsic hydrophilicity of PEO-based Pebax® 1657. Followed by PDMS coating, the water contact angle drastically increased to 115.1±2.5° because of the hydrophobic nature of PDMS.

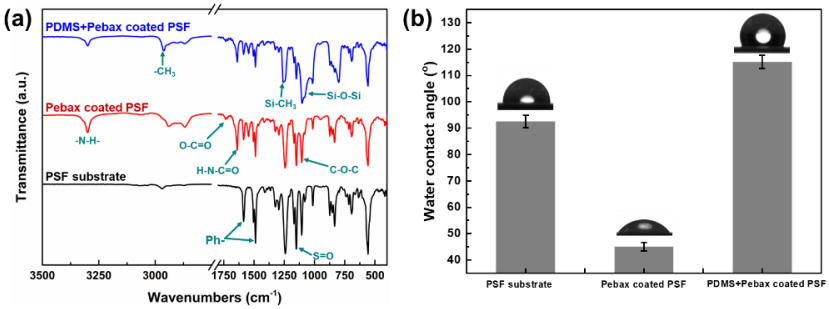

Fig.4. (a) ATR-FTIR spectra of bare PSF and Pebax spray-coated membrane. (b) Water contact angle of PSF substates and spray coated TFC membranes (the inserts represent the water contact angle snapshots of different surfaces).

3.3 Gas permeation properties of Pebax® dense membrane and PSF substrate.

The CO_2/N_2 mixed gas separation performance at 25 ℃ and 1 bar feed pressure of bare PSF substrate and dense Pebax® membrane was first investigated. As a porous substrate layer, the PSF UF membrane is expected to be extremely permeable and non-selective towards gases so as to ensure negligible mass transfer resistance. As evidenced by our performance data, the PSF substrate indeed exhibits ultrahigh CO_2 and N_2 permeance as well as an extremely low CO_2/N_2 selectivity (**Table 1**), showing a typical Knudsen diffusion gas transport behavior [66]. On the other hand, the CO_2 and N_2 permeability as well as CO_2/N_2 selectivity of Pebax® 1657 dense membrane in this work well-correspond to reported data in the literatures[27, 67, 68].

Table 1. Summary of CO_2/N_2 separation performance of PSF substrate and Pebax® 1657 dense membranes in this work and reported literatures.

Membrane type	Thickness (μm)	Permeability (barrer)		Selectivity	Ref.
		CO_2	N_2	CO_2/N_2	
PSF substrate	50	61078	51681	0.85	This work
Pebax®1657 dense membrane	40	88.1±0.5	1.56±0.1	56.9±3.9	This work
	60	78.4	1.7	46.2	[27]
	-	82	1.5	54	[67]
	64	92	2.2	42	[68]

3.4 Effect of spray volume and Pebax® concentration on membrane CO_2/N_2 separation performance.

Next, the CO_2/N_2 mixed gas separation performance of all Pebax® sprayed membranes were studied at 25 ℃ and 1 bar feed pressure. According to **Fig. 5**, a "trade-off" between gas permeance and selectivity is observed and found to be strongly dependent on the spray volume and Pebax® solution concentration. Specifically, the permeances of both CO_2 and N_2 dramatically decrease with increasing spray volume, while the CO_2/N_2 selectivity improves significantly. Meanwhile, under the same spray volume, gas permeance increases while selectivity decreases with incremental concentration of Pebax® solution.

Pebax® concentration and spray volume are closely relate to the membrane apparent thickness as well as the separation performance of the obtained TFC membranes. Generally, thinner top layer suggests higher permeance but less selective (more defective) and *vice versa*. TFC membrane (SC-PEBA$1_{0.25}$) sprayed by 0.25 mL of 1 mg/mL Pebax® solution has an ultrathin top layer that cannot fully cover the porous substrate, resulting in non-selectivity ($CO_2/N_2 \approx 0.93$) but high CO_2 (2033 GPU) and N_2 (2237 GPU) permeance. Increasing the spray volume to 0.5 mL and 1.0 mL, the CO_2 permeance of SC-PEBA$1_{0.5}$ and SC-PEBA$1_{1.0}$ markedly decreases to 334 GPU and 236 GPU, while the CO_2/N_2 selectivity jumps to 3.3 and 43.8, respectively. Likewise, increasing the concentration of Pebax® solution has similar effects. As shown in Fig. S3, at the same spray volume, the CO_2 permeance decreased while the CO_2/N_2 selectivity increased with an incremental increase in the Pebax® concentration.

Unlike conventional dip coating or doctor-blade casting, the fast and turbulent evaporation of solvent during spray coating could result in entrained air that increases the risk of defect formation. In this case, a sufficient thickness of the selective layer is necessary to reduce defects and deliver a decent CO_2/N_2 selectivity. According to **Fig. 3** and **Fig. 5**, the CO_2/N_2 selectivity of sprayed TFC membranes reached over 40 when a dense selective layer (≥100 nm) was observed (except for SC-PEBA$1_{1.0}$). Specifically, SC-PEBA$1_{1.0}$, SC-PEBA$2_{0.25}$, SC-PEBA$2_{0.5}$,

SC-PEBA$2_{1.0}$, SC-PEBA$4_{0.25}$, SC-PEBA$4_{0.5}$, and SC-PEBA$4_{1.0}$ all exhibited sufficient CO_2/N_2 selectivity (≥40). In other words, when the net amount of sprayed Pebax® is over 1 mg, a dense and defect-free selective layer can be applied on a 16 cm^2 substrate to ensure a high CO_2/N_2 selectivity. Further increasing the spray volume or Pebax concentration will increase the membrane selectivity slowly, while compromising the permeance as shown in Figs. 5b and 5c. For example, the CO_2/N_2 of SC-PEBA$4_{0.5}$ and SC-PEBA$4_{1.0}$ reached 52 and 55 with a selective layer thickness of 418 nm and 554 nm, respectively. Such CO_2/N_2 selectivity is almost similar to that of Pebax® dense membrane (see Table 1), suggesting that the selective layers are totally defect-free. However, the CO_2 permeance of SC-PEBA$4_{0.5}$ and SC-PEBA$4_{1.0}$ are only 119.5 GPU and 63.2 GPU, respectively. The high CO_2/N_2 selectivity obtained by sacrificing CO_2 permeance is not desirable. The low selectivity is most probably caused by defects in the selective layer, which means both high CO_2 permeance and high CO_2/N_2 selectivity might be achievable with thinner (≤100 nm) selective layer if defects can be properly patched.

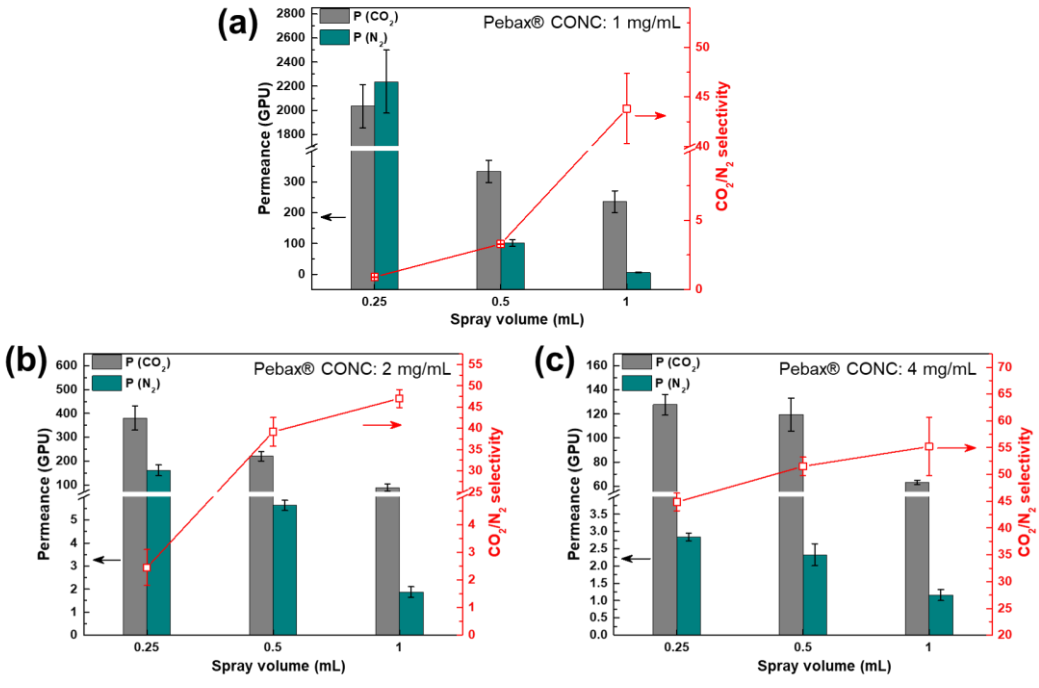

Fig.5. CO_2/N_2 mixed gas permeation performance of Pebax® sprayed membranes with different Pebax® concentration. (a) 1 mg/mL, (b) 2 mg/mL, (c) 4 mg/mL.

3.5 Effect of Post-synthesis PDMS sealing on the CO_2/N_2 separation performance of the sprayed membranes.

To further improve the performance of our spray coated Pebax® TFC membranes, we applied an additional PDMS coating on the as-prepared Pebax® TFC membranes, particularly for those with high permeance but low selectivity, aiming at patching the defects and recovering the CO_2/N_2 selectivity.

CO_2/N_2 permeation data of the membranes before and after PDMS spray are summarized in **Table 2**. Unsurprisingly, the CO_2/N_2 selectivity of PDMS coated membranes is remarkably improved, especially for those with very low pristine CO_2/N_2 selectivity before. For example, the CO_2/N_2 selectivity of SC-PEBA1$_{0.5}$ and SC-PEBA2$_{0.5}$ increased from 3.3 and 2.4 to 50.8 and 43.4 after PDMS coating, respectively. For those with decent pristine CO_2/N_2 selectivity, the PDMS coating can further improve the selectivity to more than 50, approaching the intrinsic CO_2/N_2 selectivity of Pebax® 1657. However, the increase in CO_2/N_2 selectivity still comes at the cost of compromising the CO_2 permeance. Membranes with higher pristine CO_2 permeance suffer more serious permeance loss after PDMS coating. The CO_2 permeance of SC-PEBA1$_{0.25}$ decreases by 41.9% from 380.4 GPU to 220.8 GPU while the CO_2/N_2 selectivity greatly increases by 1708%. By comparison, SC-PEBA2$_{0.5}$ only loses 8.4% of its pristine CO_2 permeance (decreases from 201.7 to 184.7) to achieve an improvement of 24.1% on its CO_2/N_2 selectivity (increases from 41.0 to 50.9).

Table 2. Comparisons of the membrane gas permeance and CO_2/N_2 selectivity before and after spray coating of PDMS protective layer.

Sample	Permeance (GPU)		Mixed gas selectivity
	CO_2	N_2	CO_2/N_2
SC-PEBA1$_{0.25}$	2033±181	2237±262	0.91±0.03
SC-PEBA2$_{0.25}$	380.4±50.7	161.7±22.4	2.4±0.7
SC-PEBA4$_{0.25}$	127.7±8.6	2.84±0.1	44.9±1.6
SC-PEBA1$_{0.5}$	334.2±35.6	101.5±11.4	3.3±0.03

SC-PEBA$2_{0.5}$	201.7±7.1	5.5±0.3	41.0±3.1
SC-PEBA$4_{0.5}$	119.5±13.8	2.3±0.3	51.5±1.7
SC-PEBA$1_{0.25}$-PDMS	1354±450	117.3±41.1	7.8±0.2
SC-PEBA$2_{0.25}$-PDMS	220.8±36.2	5.1±0.4	43.4±4.1
SC-PEBA$4_{0.25}$-PDMS	110.3±14.5	2.16±0.4	51.2±1.7
SC-PEBA$1_{0.5}$-PDMS	259.1±6.3	5.1±0.2	50.8±0.7
SC-PEBA$2_{0.5}$-PDMS	184.7±4.6	3.6±0.04	50.9±1.3
SC-PEBA$4_{0.5}$-PDMS	95.5±3.0	1.8±0.09	53.9±1.4

The benefits brought by additional PDMS coating are not limited to selectivity recovery. We further investigated the CO_2/N_2 mixed gas separation performance under incremental feed pressure with results as shown in **Fig. 6**. Both CO_2 permeance and CO_2/N_2 selectivity for each membrane gradually decreases with increasing feed pressure, while N_2 permeance shows only a slight increase (**Fig. 6a**). We believe that the opposite trend demonstrated by the change in CO_2 and N_2 permeance is a result of CO_2 plasticization effect and competitive gas adsorption effect counteracting one another, which is in good agreement to the literatures [69, 70]. In general, enhancing the feed pressure will significantly increase the solubility of CO_2 in polymers, especially for those CO_2-philic PEO-based polymers [71-74]. Large amount of CO_2 condensation will in turn plasticize the polymer, leading to expanded free volume and increased chain mobility. Normally, plasticization effect is more noticeable for thinner membranes and at lower applied pressures, which result in enhanced CO_2 permeability under pure gas test condition [74-76]. However, when using mixed gas comprising 80% inert N_2 and 20% CO_2 as test feed, the transport of N_2 can also be facilitated by plasticization effect since the larger gas molecules can also leverage the enhanced free volume and chain mobility to increase its diffusion [77]. Hence, CO_2 plasticization is counterbalanced by the competitive adsorption of N_2 molecules, which effect is stronger at higher feed pressure [70]. Consequently, CO_2 permeance decreases while N_2 permeance is enhanced with increasing feed pressure. For PDMS

coated membranes, the drop in CO_2 permeance and CO_2/N_2 selectivity as well as the increase in N_2 permeance during higher feed pressure are observably suppressed (**Fig. 6b**). In other words, PDMS coating can strengthen CO_2 plasticization resistance of the sprayed Pebax® TFC membranes, which is conductive to maintain the membrane performance under high pressure conditions.

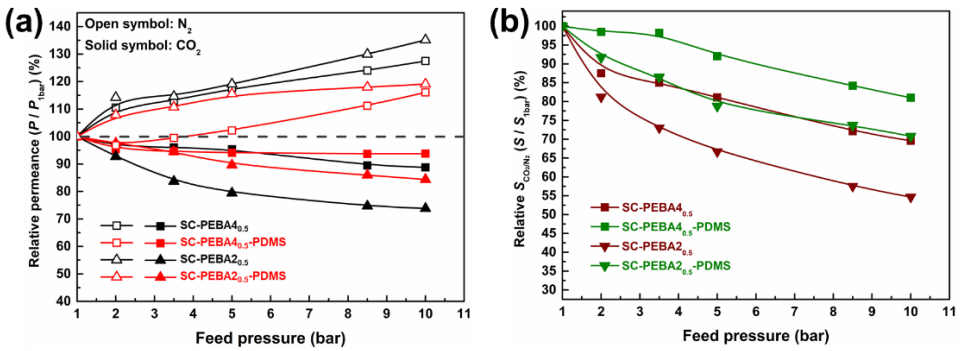

Fig. 6. Membrane CO_2/N_2 mixed gas separation performance under different feed pressure, (a) CO_2 and N_2 permeance, (b) CO_2/N_2 selectivity.

3.6. Scaled-up demonstration of the direct-sprayed Pebax® TFC membrane

The Pebax® TFC membrane was further fabricated on an A4-sized PSF substrate (**Fig. 7**) to demonstrate the scaled-up potential of the direct spray-coating strategy. The A4-sized membrane was fabricated by manually spraying 40 mL Pebax® solution (1 mg/mL) on the PSF substrate at a speed of 5 mL/min. After drying and the deposition of a PDMS protective layer, the CO_2/N_2 separation performance was evaluated by testing 10 randomly selected samples cut from the as-prepared A4-sized membrane on a laboratory-scale permeation cell. As summarized in **Table 3**, the A4-sized membrane exhibits an average CO_2 permeance of 188.5 GPU and an average CO_2/N_2 selectivity of 42.4, which are acceptable though slightly lower than the performance of coupon-sized membranes evaluated in Section 3.5. The relatively lower performance is ascribed to the nonuniformity spraying under manual operation and increased defects occurrence rate with a large-area spray, which can be addressed by machine spraying in future study. Overall, the successful fabrication of the A4-sized membrane demonstrates the

356 excellent reproducibility and great scaled-up potential of our direct spray-coating method.

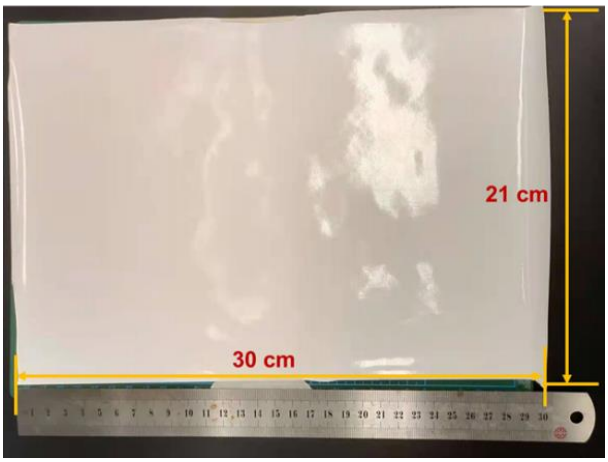

357

358 **Fig. 7.** Photograph of the Pebax®1657 spray-coated A4-sized membrane.

359 **Table 3.** CO_2/N_2 mixed gas permeation results, average data, and standard deviations of the
360 A4-sized TFC membrane

	Sample No.	Permeance (GPU)		Mixed gas selectivity
		N_2	CO_2	CO_2/N_2
	1	3.4	151.2	44.3
	2	3.6	155.5	43.5
	3	8.0	221.6	40.2
	4	5.9	261.3	44.4
	5	4.2	179.7	42.9
	6	4.0	177.3	43.8
	7	4.3	198.6	45.8
	8	4.8	196.3	45.8
	9	4.5	168.6	37.7
	10	4.9	175.2	35.6
Average		4.8	188.5	42.4
Standard deviation		1.3	31.3	3.3

361

3.7. Long-term stability and the performance comparison with reported TFC membranes

The long-term CO_2/N_2 mixed gas permeation test was carried at 25 ℃ and 1 bar under a continuous transmembrane gas flow to investigate the performance stability of the sprayed membrane. The as-prepared SC-PEBA$1_{0.5}$-PDMS exhibited a relatively stable long-term performance for 100-hour consecutive test running at 1bar and 25 ℃ (**Fig. 8**), during which the CO_2 permeance and CO_2/N_2 selectivity slightly fluctuated around 220 GPU and 45, respectively.

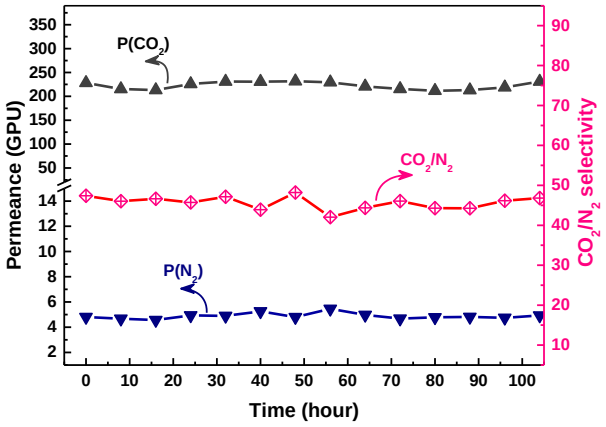

Fig. 8. CO_2/N_2 mixed gas permeation long-term stability test results including CO_2 permeance, N_2 permeance, and CO_2/N_2 selectivity of SC-PEBA$1_{0.5}$-PDMS at 1 bar and 25 ℃.

The direct sprayed Pebax® membranes in this work show comparable CO_2/N_2 separation performance with the reported Pebax®-based TFC membranes as shown in **Fig.9** and **Table S1**. Clearly, the CO_2 permeance of our direct sprayed TFC membrane is much higher than those PEO-based TFC membranes without gutter layers but has little advantages to TFC membranes with gutter layers. Although the CO_2 permeance of this work is moderate, the direct spray coating method has its own advantages, including low cost, facile fabrication (without gutter layer), and easy scale-up, over other state-of-the-art membranes such as facilitated transport and nanocomposite membranes. Our A4-sized membrane demonstration has also provided evidence-based scalability potential, rendering our direct sprayed membranes attractive and relevant for industrial CO_2 capture applications.

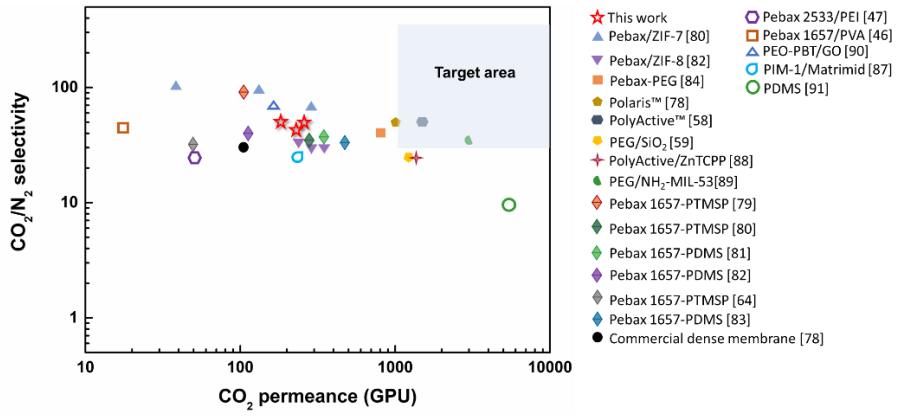

Fig. 9. The CO_2/N_2 separation performance of direct sprayed Pebax® membranes in this work in comparison with reported TFC membranes and commercial dense membrane (Solid symbols represent the TFC membranes with gutter layers, open symbols represent the TFC membranes without gutter layers). The target area is proposed by Merkel et al.[78]. The CO_2/N_2 separation performance of other reported membranes are extracted from literatures[46, 47, 64, 78-91].

4. Conclusion and perspective

A facile direct spray-coating method was successfully developed in this work to fabricate Pebax® 1657 TFC membrane for CO_2 capture. The removal of the need for a gutter layer and the use of a commercially available polymer significantly simplify the membrane fabrication protocol, which could potentially help save costs. The separation performance of the direct sprayed TFC membranes is well-correlated to the concentration of the Pebax solution and the spray volume, given that CO_2 permeance decreased while CO_2/N_2 selectivity increased with increasing Pebax concentration and spray volume. By adjusting the separation parameters, TFC membranes with CO_2 permeance in the range of 63.2 GPU to 235.6 GPU and CO_2/N_2 selectivity of over 40 could be obtained. By applying an extra PDMS sealing coating, the optimized membrane, SC-PEBA$1_{0.5}$-PDMS, can reach a CO_2 permeance of 259.1 GPU and a CO_2/N_2 selectivity of 50.8. Additionally, the membrane fabrication can be easily scaled-up to A4-size using laboratory-scale equipment. We believe that the large-scale replication of the

sprayed membrane is within reach if we transit to machine spray coating in the future study."

However, due to the relatively lower CO_2 permeance, the direct spray coating method may not as attractive as other conventional methods at the current stage. Before the practical implementation of the spray coating method, several problems, including the low use ratio of spray solution, the spray uniformity, and the extent of intrusion of the spray solution, need to be further addressed. So far, a gutter layer seems unavoidable for achieving high permeance TFC membranes. Hence, as a future work, gutter layer can also be introduced by spray coating to further elevate the performance of spray coated TFC membranes. Overall, the spray coating method has shown great promise to be a versatile platform for designing state-of-the-art thin-film composite membranes by enabling high-performance materials (polymers/additives) to be easily processable as the selective layer at a membrane area potentially close to the industrial-scale.

Acknowledgements

The authors would like to acknowledgement the Singapore Membrane Technology center, Nanyang Environment and Water Research Institute, Nanyang Technological University, and the financial support of Economic Development Board of Singapore.

Author statements

Xu Jiang: Conceptualization, Investigation, Methodology, Formal analysis, Writing-Original Draft, Writing-Review and Editing.

Chong Yang Chuah: Methodology.

Kunli Goh: Writing-review & editing

Rong Wang: Supervision, Writing-Review & Editing, Funding acquisition.

Declaration of competing interests

The authors declare that they have no known competing financial interests or personal relationships that could have appeared to influence the work reported in this paper.

Reference

[1] M.R. Smith, S.S. Myers, Impact of anthropogenic CO_2 emissions on global human nutrition, Nat. Clim. Change, 8 (2018) 834-839.

[2] C. Zhu, K. Kobayashi, I. Loladze, J. Zhu, Q. Jiang, X. Xu, G. Liu, S. Seneweera, K.L. Ebi, A. Drewnowski, N.K. Fukagawa, L.H. Ziska, Carbon dioxide (CO_2) levels this century will alter the protein, micronutrients, and vitamin content of rice grains with potential health consequences for the poorest rice-dependent countries, Sci. Adv., 4 (2018) eaaq1012.

[3] M. Bui, C.S. Adjiman, A. Bardow, E.J. Anthony, A. Boston, S. Brown, P.S. Fennell, S. Fuss, A. Galindo, L.A. Hackett, J.P. Hallett, H.J. Herzog, G. Jackson, J. Kemper, S. Krevor, G.C. Maitland, M. Matuszewski, I.S. Metcalfe, C. Petit, G. Puxty, J. Reimer, D.M. Reiner, E.S. Rubin, S.A. Scott, N. Shah, B. Smit, J.P.M. Trusler, P. Webley, J. Wilcox, N. Mac Dowell, Carbon capture and storage (CCS): the way forward, Energy Environ. Sci., 11 (2018) 1062-1176.

[4] L. Rosa, J.A. Reimer, M.S. Went, P. D'Odorico, Hydrological limits to carbon capture and storage, Nat. Sustain., 3 (2020) 658-666.

[5] X.Q. Cheng, Z.X. Wang, X. Jiang, T. Li, C.H. Lau, Z. Guo, J. Ma, L. Shao, Towards sustainable ultrafast molecular-separation membranes: From conventional polymers to emerging materials, Prog. Mater. Sci., 92 (2018) 258-283.

[6] H.B. Park, J. Kamcev, L.M. Robeson, M. Elimelech, B.D. Freeman, Maximizing the right stuff: The trade-off between membrane permeability and selectivity, Science, 356 (2017).

[7] R.W. Baker, B.T. Low, Gas Separation Membrane Materials: A Perspective, Macromolecules, 47 (2014) 6999-7013.

[8] R.W. Baker, Membrane technology and applications, John Wiley & Sons, Ltd, (2004) 96-103.

[9] S.L. Liu, L. Shao, M.L. Chua, C.H. Lau, H. Wang, S. Quan, Recent progress in the design of advanced PEO-containing membranes for CO_2 removal, Prog. Polym. Sci., 38 (2013) 1089-1120.

[10] Z. Tong, W.S.W. Ho, Facilitated transport membranes for CO_2 separation and capture, Separ. Sci. Technol., 52 (2016) 156-167.

[11] K.M. Gupta, Y. Chen, J. Jiang, Ionic Liquid Membranes Supported by Hydrophobic and Hydrophilic Metal–Organic Frameworks for CO_2 Capture, J. Phys. Chem. C, 117 (2013) 5792-5799.

[12] J.G. Vitillo, M. Savonnet , G. Ricchiardi, S. Bordiga, Tailoring Metal–Organic Frameworks for CO_2 Capture: The Amino Effect, ChemSusChem, 4 (2011) 1281-1290.

[13] Y. Zeng, R. Zou, Y. Zhao, Covalent Organic Frameworks for CO_2 Capture, Adv. Mater., 28 (2016) 2855-2873.

[14] N. Huang, X. Chen, R. Krishna, D. Jiang, Two-dimensional covalent organic frameworks for carbon dioxide capture through channel-wall functionalization, Angew. Chem. Int. Ed., 54 (2015) 2986-2990.

[15] J. Shen, G. Liu, K. Huang, W. Jin, K.R. Lee, N. Xu, Membranes with fast and selective gas-transport channels of laminar graphene oxide for efficient CO_2 capture, Angew. Chem. Int. Ed., 54 (2015) 578-582.

[16] M. Wang, Z. Wang, S. Li, C. Zhang, J. Wang, S. Wang, A high performance antioxidative and acid resistant membrane prepared by interfacial polymerization for CO_2 separation from flue gas, Energy Environ. Sci., 6 (2013) 539-551.

[17] S.F. Wang, X.Q. Li, H. Wu, Z.Z. Tian, Q.P. Xin, G.W. He, D.D. Peng, S.L. Chen, Y. Yin, Z.Y. Jiang, M.D. Guiver, Advances in high permeability polymer-based membrane materials

for CO_2 separations, Energy Environ. Sci., 9 (2016) 1863-1890.

[18] M. Shah, M.C. McCarthy, S. Sachdeva, A.K. Lee, H.-K. Jeong, Current Status of Metal–Organic Framework Membranes for Gas Separations: Promises and Challenges, Ind. Eng. Chem. Res., 51 (2012) 2179-2199.

[19] Z. Kang, L. Fan, D. Sun, Recent advances and challenges of metal-organic framework membranes for gas separation, J. Mater. Chem. A, 5 (2017) 10073-10091.

[20] N. Kosinov, J. Gascon, F. Kapteijn, E.J.M. Hensen, Recent developments in zeolite membranes for gas separation, J. Membr. Sci., 499 (2016) 65-79.

[21] H. Lin, E. Van Wagner, B.D. Freeman, L.G. Toy, R.P. Gupta, Plasticization-Enhanced Hydrogen Purification Using Polymeric Membranes, Science, 311 (2006) 639-642.

[22] H. Lin, B.D. Freeman, Gas solubility, diffusivity and permeability in poly(ethylene oxide), J. Membr. Sci., 239 (2004) 105-117.

[23] S. Quan, Y.P. Tang, Z.X. Wang, Z.X. Jiang, R.G. Wang, Y.Y. Liu, L. Shao, PEG-Imbedded PEO Membrane Developed by a Novel Highly Efficient Strategy Toward Superior Gas Transport Performance, Macromol. Rapid Commun., 36 (2015) 490-495.

[24] L. Shao, T.-S. Chung, In situ fabrication of cross-linked PEO/silica reverse-selective membranes for hydrogen purification, Int. J. Hydrogen Energy, 34 (2009) 6492-6504.

[25] I. Hossain, A. Husna, S. Chaemchuen, F. Verpoort, T.H. Kim, Cross-Linked Mixed-Matrix Membranes Using Functionalized UiO-66-NH_2 into PEG/PPG-PDMS-Based Rubbery Polymer for Efficient CO_2 Separation, ACS Appl. Mater. Interfaces, 12 (2020) 57916-57931.

[26] B. Zhu, X. Jiang, S. He, X. Yang, J. Long, Y. Zhang, L. Shao, Rational design of poly(ethylene oxide) based membranes for sustainable CO_2 capture, J. Mater. Chem. A, 8 (2020) 24233-24252.

[27] N. Habib, Z. Shamair, N. Tara, A.-S. Nizami, F.H. Akhtar, N.M. Ahmad, M.A. Gilani, M.R. Bilad, A.L. Khan, Development of highly permeable and selective mixed matrix membranes based on Pebax®1657 and NOTT-300 for CO_2 capture, Sep. Purif. Technol., 234 (2020).

505 [28] P.D. Sutrisna, J. Hou, M.Y. Zulkifli, H. Li, Y. Zhang, W. Liang, D. D'Alessandro, V. Chen,
506 Surface functionalized UiO-66/Pebax-based ultrathin composite hollow fiber gas separation
507 membranes, J. Mater. Chem. A, 6 (2018) 918-931.
508 [29] L.S. White, K.D. Amo, T. Wu, T.C. Merkel, Extended field trials of Polaris sweep modules
509 for carbon capture, J. Membr. Sci., 542 (2017) 217-225.
510 [30] H. Lin, Z. He, Z. Sun, J. Vu, A. Ng, M. Mohammed, J. Kniep, T.C. Merkel, T. Wu, R.C.
511 Lambrecht, CO_2-selective membranes for hydrogen production and CO_2 capture-Part I:
512 Membrane development, J. Membr. Sci., 457 (2014) 149-161.
513 [31] T. Brinkmann, J. Lillepärg, H. Notzke, J. Pohlmann, S. Shishatskiy, J. Wind, T. Wolff,
514 Development of CO_2 Selective Poly(Ethylene Oxide)-Based Membranes: From Laboratory to
515 Pilot Plant Scale, Engineering, 3 (2017) 485-493.
516 [32] M.M. Rahman, C. Abetz, S. Shishatskiy, J. Martin, A.J. Muller, V. Abetz, CO_2 Selective
517 PolyActive Membrane: Thermal Transitions and Gas Permeance as a Function of Thickness,
518 ACS Appl. Mater. Interfaces, 10 (2018) 26733-26744.
519 [33] Y. Ji, M. Zhang, K. Guan, J. Zhao, G. Liu, W. Jin, High-Performance CO_2 Capture through
520 Polymer-Based Ultrathin Membranes, Adv. Funct. Mater., 29 (2019) 1900735.
521 [34] O. Selyanchyn, R. Selyanchyn, S. Fujikawa, Critical Role of the Molecular Interface in
522 Double-Layered Pebax-1657/PDMS Nanomembranes for Highly Efficient CO_2/N_2 Gas
523 Separation, ACS Appl. Mater. Interfaces, 12 (2020) 33196-33209.
524 [35] M. Liu, M.D. Nothling, P.A. Webley, Q. Fu, G.G. Qiao, Postcombustion Carbon Capture
525 Using Thin-Film Composite Membranes, Acc Chem Res, 52 (2019) 1905-1914.
526 [36] C.Z. Liang, T.-S. Chung, J.-Y. Lai, A review of polymeric composite membranes for gas
527 separation and energy production, Prog. Polym. Sci., 97 (2019).
528 [37] Z. Dai, L. Ansaloni, L. Deng, Recent advances in multi-layer composite polymeric
529 membranes for CO_2 separation: A review, Green Energy Environ., 1 (2016) 102-128.
530 [38] K. Xie, Q. Fu, G.G. Qiao, P.A. Webley, Recent progress on fabrication methods of
531 polymeric thin film gas separation membranes for CO_2 capture, J. Membr. Sci., 572 (2019) 38-

60.

[39] X. He, A. Lindbråthen, T.-J. Kim, M.-B. Hägg, Pilot testing on fixed-site-carrier membranes for CO_2 capture from flue gas, Int. J. Greenh. Gas Con., 64 (2017) 323-332.

[40] Z. Dai, S. Fabio, N. Giuseppe Marino, C. Riccardo, L. Deng, Field test of a pre-pilot scale hollow fiber facilitated transport membrane for CO_2 capture, Int. J. Greenh. Gas Con., 86 (2019) 191-200.

[41] M. Cook, P.R.J. Gaffney, L.G. Peeva, A.G. Livingston, Roll-to-roll dip coating of three different PIMs for Organic Solvent Nanofiltration, J. Membr. Sci., 558 (2018) 52-63.

[42] M.M. Rahman, C. Abetz, S. Shishatskiy, J. Martin, A.J. Müller, V. Abetz, CO_2 Selective PolyActive Membrane: Thermal Transitions and Gas Permeance as a Function of Thickness, ACS Appl. Mater. Interfaces, 10 (2018) 26733-26744.

[43] M.J. Yoo, K.H. Kim, J.H. Lee, T.W. Kim, C.W. Chung, Y.H. Cho, H.B. Park, Ultrathin gutter layer for high-performance thin-film composite membranes for CO_2 separation, J. Membr. Sci., 566 (2018) 336-345.

[44] M. Kattula, K. Ponnuru, L. Zhu, W. Jia, H. Lin, E.P. Furlani, Designing ultrathin film composite membranes: the impact of a gutter layer, Scientific Reports, 5 (2015) 15016.

[45] M. Mozafari, R. Abedini, A. Rahimpour, Zr-MOFs-incorporated thin film nanocomposite Pebax 1657 membranes dip-coated on polymethylpentyne layer for efficient separation of CO_2/CH_4, J. Mater. Chem. A, 6 (2018) 12380-12392.

[46] K.C. Wong, P.S. Goh, A.F. Ismail, Enhancing hydrogen gas separation performance of thin film composite membrane through facilely blended polyvinyl alcohol and PEBAX, Int. J. Hydrogen Energy, 46 (2021) 19737-19748.

[47] L. Liu, A. Chakma, X. Feng, CO_2/N_2 Separation by Poly(Ether Block Amide) Thin Film Hollow Fiber Composite Membranes, Ind. Eng. Chem. Res., 44 (2005) 6874-6882.

[48] E. Esposito, G. Clarizia, P. Bernardo, J.C. Jansen, Z. Sedláková, P. Izák, S. Curcio, B.d. Cindio, F. Tasselli, Pebax®/PAN hollow fiber membranes for CO_2/CH_4 separation, Chem. Eng. Process., 94 (2015) 53-61.

559 [49] C. Cheng, D. Yang, M. Bao, C. Xue, Spray-coated PDMS/PVDF composite membrane for
560 enhanced butanol recovery by pervaporation, J. Appl. Polym. Sci., 138 (2021) 49738.
561 [50] H. Tang, S. Ji, L. Gong, H. Guo, G. Zhang, Tubular ceramic-based multilayer separation
562 membranes using spray layer-by-layer assembly, Polym. Chem., 4 (2013) 5621-5628.
563 [51] C. Jiao, Z. Li, X. Li, M. Wu, H. Jiang, Improved CO_2/N_2 separation performance of Pebax
564 composite membrane containing polyethyleneimine functionalized ZIF-8, Sep. Purif. Technol.,
565 259 (2021) 118190.
566 [52] H. Tang, G. Zhang, S. Ji, Rapid assembly of polyelectrolyte multilayer membranes using
567 an automatic spray system, AIChE J.59 (2013) 250-257.
568 [53] K.L. Cho, H. Lomas, A.J. Hill, F. Caruso, S.E. Kentish, Spray Assembled, Cross-Linked
569 Polyelectrolyte Multilayer Membranes for Salt Removal, Langmuir, 30 (2014) 8784-8790.
570 [54] K.C. Krogman, J.L. Lowery, N.S. Zacharia, G.C. Rutledge, P.T. Hammond, Spraying
571 asymmetry into functional membranes layer-by-layer, Nat. Mater, 8 (2009) 512-518.
572 [55] K. Guan, J. Shen, G. Liu, J. Zhao, H. Zhou, W. Jin, Spray-evaporation assembled graphene
573 oxide membranes for selective hydrogen transport, Sep. Purif. Technol., 174 (2017) 126-135.
574 [56] W. Wei, W. Zhang, Q. Jiang, P. Xu, Z. Zhong, F. Zhang, W. Xing, Preparation of non-
575 oxide SiC membrane for gas purification by spray coating, J. Membr. Sci., 540 (2017) 381-390.
576 [57] J. Heo, M. Choi, D. Choi, H. Jeong, H.Y. Kim, H. Jeon, S.W. Kang, J. Hong, Spray-
577 assisted layer-by-layer self-assembly of tertiary-amine-stabilized gold nanoparticles and
578 graphene oxide for efficient CO_2 capture, J. Membr. Sci., 601 (2020) 117905.
579 [58] V.M. Aceituno Melgar, H.T. Kwon, J. Kim, Direct spraying approach for synthesis of ZIF-
580 7 membranes by electrospray deposition, J. Membr. Sci., 459 (2014) 190-196.
581 [59] Z. Yali, L.G. Sung, W. Yining, L. Can, W. Rong, Impact of pilot-scale PSF substrate
582 surface and pore structural properties on tailoring seawater reverse osmosis membrane
583 performance, J. Membr. Sci., 633 (2021) 119395.
584 [60] J. Park, H.W. Yoon, D.R. Paul, B.D. Freeman, Gas transport properties of PDMS-coated
585 reverse osmosis membranes, J. Membr. Sci., 604 (2020).

[61] S. Lashkari, A. Tran, B. Kruczek, Effect of back diffusion and back permeation of air on membrane characterization in constant pressure system, J. Membr. Sci., 324 (2008) 162-172.

[62] F.V. Adams, E.N. Nxumalo, R.W.M. Krause, E.M.V. Hoek, B.B. Mamba, Preparation and characterization of polysulfone/β-cyclodextrin polyurethane composite nanofiltration membranes, J. Membr. Sci., 405-406 (2012) 291-299.

[63] S.R. Kim, K.H. Lee, M.S. Jhon, The effect of $ZnCl_2$ on the formation of polysulfone membrane, J. Membr. Sci., 119 (1996) 59-64.

[64] W. Fam, J. Mansouri, H. Li, V. Chen, Improving CO_2 separation performance of thin film composite hollow fiber with Pebax®1657/ionic liquid gel membranes, J. Membr. Sci., 537 (2017) 54-68.

[65] M.R. Moradi, M. Pourafshari Chenar, S.H. Noie, M. Hesampour, M. Mänttäri, PDMS coating of used TFC-RO membranes for O_2/N_2 and CO_2/N_2 gas separation applications, Polym Test, 63 (2017) 101-109.

[66] R. Pang, K.K. Chen, Y. Han, W.S.W. Ho, Highly permeable polyethersulfone substrates with bicontinuous structure for composite membranes in CO_2/N_2 separation, J. Membr. Sci., 612 (2020).

[67] H. Wu, X. Li, Y. Li, S. Wang, R. Guo, Z. Jiang, C. Wu, Q. Xin, X. Lu, Facilitated transport mixed matrix membranes incorporated with amine functionalized MCM-41 for enhanced gas separation properties, J. Membr. Sci., 465 (2014) 78-90.

[68] G. Huang, A.P. Isfahani, A. Muchtar, K. Sakurai, B.B. Shrestha, D. Qin, D. Yamaguchi, E. Sivaniah, B. Ghalei, Pebax/ionic liquid modified graphene oxide mixed matrix membranes for enhanced CO_2 capture, J. Membr. Sci., 565 (2018) 370-379.

[69] A. Car, C. Stropnik, W. Yave, K.-V. Peinemann, Pebax®/polyethylene glycol blend thin film composite membranes for CO_2 separation: Performance with mixed gases, Sep. Purif. Technol., 62 (2008) 110-117.

[70] T. Visser, G.H. Koops, M. Wessling, On the subtle balance between competitive sorption and plasticization effects in asymmetric hollow fiber gas separation membranes, J. Membr. Sci.,

613 252 (2005) 265-277.
614 [71] S.R. Reijerkerk, K. Nijmeijer, C.P. Ribeiro, B.D. Freeman, M. Wessling, On the effects of
615 plasticization in CO_2/light gas separation using polymeric solubility selective membranes, J.
616 Membr. Sci., 367 (2011) 33-44.
617 [72] L. Huang, J. Liu, H. Lin, Thermally stable, homogeneous blends of cross-linked
618 poly(ethylene oxide) and crown ethers with enhanced CO_2 permeability, J. Membr. Sci., 610
619 (2020).
620 [73] N.U. Kim, B.J. Park, M.D. Guiver, J.H. Kim, Use of non-selective, high-molecular-weight
621 poly(ethylene oxide) membrane for CO_2 separation by incorporation of comb copolymer, J.
622 Membr. Sci., 605 (2020).
623 [74] R.R. Tiwari, J. Jin, B.D. Freeman, D.R. Paul, Physical aging, CO_2 sorption and
624 plasticization in thin films of polymer with intrinsic microporosity (PIM-1), J. Membr. Sci.,
625 537 (2017) 362-371.
626 [75] X. Jiang, S. Li, S. He, Y. Bai, L. Shao, Interface manipulation of CO_2-philic composite
627 membranes containing designed UiO-66 derivatives towards highly efficient CO_2 capture, J.
628 Mater. Chem. A, 6 (2018) 15064-15073.
629 [76] X. Jiang, S. He, S. Li, Y. Bai, L. Shao, Penetrating chains mimicking plant root branching
630 to build mechanically robust, ultra-stable CO_2-philic membranes for superior carbon capture, J.
631 Mater. Chem. A, 7 (2019) 16704-16711.
632 [77] X. Jiang, S. Li, L. Shao, Pushing CO_2-philic membrane performance to the limit by
633 designing semi-interpenetrating networks (SIPN) for sustainable CO_2 separations, Energy
634 Environ. Sci., 10 (2017) 1339-1344.
635 [78] T.C. Merkel, H.Q. Lin, X.T. Wei, R. Baker, Power plant post-combustion carbon dioxide
636 capture: An opportunity for membranes, J. Membr. Sci., 359 (2010) 126-139.
637 [79] Y. Wang, T. Hu, H. Li, G. Dong, W. Wong, V. Chen, Enhancing Membrane Permeability
638 for CO_2 Capture Through Blending Commodity Polymers with Selected PEO and PEO-PDMS
639 Copolymers and Composite Hollow Fibres, Energy Procedia, 63 (2014) 202-209.

[80] T. Li, Y. Pan, K.-V. Peinemann, Z. Lai, Carbon dioxide selective mixed matrix composite membrane containing ZIF-7 nano-fillers, J. Membr. Sci., 425-426 (2013) 235-242.

[81] H.Z. Chen, Z. Thong, P. Li, T.-S. Chung, High performance composite hollow fiber membranes for CO_2/H_2 and CO_2/N_2 separation, Int. J. Hydrogen Energy, 39 (2014) 5043-5053.

[82] P.D. Sutrisna, J. Hou, H. Li, Y. Zhang, V. Chen, Improved operational stability of Pebax-based gas separation membranes with ZIF-8: A comparative study of flat sheet and composite hollow fibre membranes, J. Membr. Sci., 524 (2017) 266-279.

[83] J.M.P. Scofield, P.A. Gurr, J. Kim, Q. Fu, S.E. Kentish, G.G. Qiao, Blends of Fluorinated Additives with Highly Selective Thin-Film Composite Membranes to Increase CO_2 Permeability for CO_2/N_2 Gas Separation Applications, Ind. Eng. Chem. Res., 55 (2016) 8364-8372.

[84] J. Lillepärg, P. Georgopanos, T. Emmler, S. Shishatskiy, Effect of the reactive amino and glycidyl ether terminated polyethylene oxide additives on the gas transport properties of Pebax® bulk and thin film composite membranes, RSC Adv., 6 (2016) 11763-11772.

[85] W. Yave, H. Huth, A. Car, C. Schick, Peculiarity of a CO_2-philic block copolymer confined in thin films with constrained thickness: “a super membrane for CO_2-capture”, Energy Environ. Sci., 4 (2011).

[86] J. Kim, Q. Fu, K. Xie, J.M.P. Scofield, S.E. Kentish, G.G. Qiao, CO_2 separation using surface-functionalized SiO2 nanoparticles incorporated ultra-thin film composite mixed matrix membranes for post-combustion carbon capture, J. Membr. Sci., 515 (2016) 54-62.

[87] W.F. Yong, F.Y. Li, Y.C. Xiao, T.S. Chung, Y.W. Tong, High performance PIM-1/Matrimid hollow fiber membranes for CO_2/CH_4, O_2/N_2 and CO_2/N_2 separation, J. Membr. Sci., 443 (2013) 156-169.

[88] M. Liu, K. Xie, M.D. Nothling, P.A. Gurr, S.S.L. Tan, Q. Fu, P.A. Webley, G.G. Qiao, Ultrathin Metal-Organic Framework Nanosheets as a Gutter Layer for Flexible Composite Gas Separation Membranes, ACS Nano, 12 (2018) 11591-11599.

[89] K. Xie, Q. Fu, C. Xu, H. Lu, Q. Zhao, R. Curtain, D. Gu, P.A. Webley, G.G. Qiao,

667 Continuous assembly of a polymer on a metal–organic framework (CAP on MOF): a 30 nm
668 thick polymeric gas separation membrane, Energy Environ. Sci., 11 (2018) 544-550.
669 [90] M. Karunakaran, R. Shevate, M. Kumar, K.V. Peinemann, CO_2-selective PEO–PBT
670 (PolyActive™)/graphene oxide composite membranes, Chem. Commun., 51 (2015) 14187-
671 14190.
672 [91] C.Z. Liang, W.F. Yong, T.-S. Chung, High-performance composite hollow fiber
673 membrane for flue gas and air separations, J. Membr. Sci., 541 (2017) 367-377.